

3D Cell Arrangement and Its Pathologic Change

Hideo Shimizu

Department of Pathology, Shonan Atsugi Hospital, Nurumizu, Atsugi, Kanagawa 243-8551, Japan
E-mail address: hshimizu@shonan-atsugi.jp

(Received October 15, 2011; Accepted March 15, 2012)

3D shapes of biological cells and their arrangement were discussed. The positional relationship between cell arrangement and blood vessels was studied, and it was found that the blood vessels go along some edges of the cells in the tissue. A quantitative topological analysis of the 3D microvascular network of the liver, i.e. hepatic sinusoids, was performed with the aid of a computer system for reconstruction from serial tissue sections. The pathologic change of the sinusoids (vascular channels between the liver cell plates) in cirrhosis (hard liver with nodular surface) and hepatocellular carcinoma (primary malignant epithelial tumor of the liver) was also studied. There was a statistically significant difference of the first Betti number, p_1 , of the sinusoids in the three groups, the two pathologic cases and normal one. A 2D index was proposed, based on the results from the reconstruction study and Alexander duality theorem in topology, to perform rapid structural analysis of the 3D sinusoidal network. It was concluded that the 2D index was useful for estimating the complexity degree of the 3D sinusoidal network.

Key words: 3D Cell Arrangement, Topology, Alexander Duality Theorem, Hepatic Sinusoids, Pathologic Change

1. Introduction

There are two different types of cells in the body: epithelial cells and non-epithelial ones. The epithelial cells cover the free surfaces of the body, varying from the exposed external surface to the smallest free facets within the internal organs. At least one face of each epithelial cell, other than stratified epithelium (epithelial cell sheet having two or more cell layers), looks towards an external space or an internal lumen (inner space), and another face looks towards a supporting extracellular matrix, the basement membrane. Each epithelial cell therefore has the apical to basal direction, i.e. it has a polarity. The remaining faces directly cohere adjacent epithelial cells. On the other hand, non-epithelial cells have no face looking towards the external space or the internal lumen. All the faces of the non-epithelial cells look towards the connective tissue, extracellular matrix. Each non-epithelial cell has no polarity.

1.1 Epithelial cell

The glandular epithelial cell, forming glands (aggregation of cells specialized to secrete or excrete materials), produces substances in the cell and excretes them into the extracellular space. The excreted fluid goes into the adjacent duct, whose inner surface covered by epithelial cells, and is transported to the internal lumen. The size of the space in the center of the glands or of the tube is similar to that of their epithelial cells, or larger than that of them. A face of each glandular epithelial cell or ductal epithelial one therefore looks towards the space, and another face looks towards the basal layer, and the remaining faces front the adjacent epithelial cells (Fig. 1). Then the 3D shape of most

of the epithelial cells is hexagonal prism (Fig. 2).

1.2 Non-epithelial cell

Non-epithelial cells, such as fibroblasts or chondrocytes, are usually discretely distributed in the extracellular matrix (Fig. 3). Skeletal muscle is also non-epithelial, and consists of long bundles of more or less parallel cells called muscle fibers. The photomicrograph of skeletal muscle fibers in cross section illustrates their polygonal outline (Fig. 4). Hexagons predominate among the polygons.

1.3 Topology of plane division

Among polygonal cells, not only epithelial but also non-epithelial ones, which are packing a plane, the hexagons predominate. This can be proved by the use of topology.

When a plane is divided by polygons, the number of polygons F , the number of edges E and the number of vertices V give the Euler-Poincaré characteristic denoted by χ , as follows (Coxeter, 1989a):

$$\chi = F - E + V, \quad (1)$$

where $\chi = 2$ for a spherical surface, $\chi = 1$ for a flat plane and $\chi = 0$ for a torus surface.

We assume further that F polygons include f_i i -sided polygons ($i = 3, 4, \dots$), then we have $\sum f_i = F$. Let p_i be the probability of the existence of i -sided polygons, then p_i is f_i/F and $\sum i \cdot f_i = 2E$. In the same way, let v_j be the number of edges joining a vertex ($j = 3, 4, \dots$), then we have $\sum j \cdot v_j = 2E$. In a stable cell division, the number of edges joining every vertex is three, hence $V = v_3$, and $3 \cdot v_3 = 2E$.

We can prove that the average of i converges to 6 for large number of F . Put the above relations into Eq. (1), then we

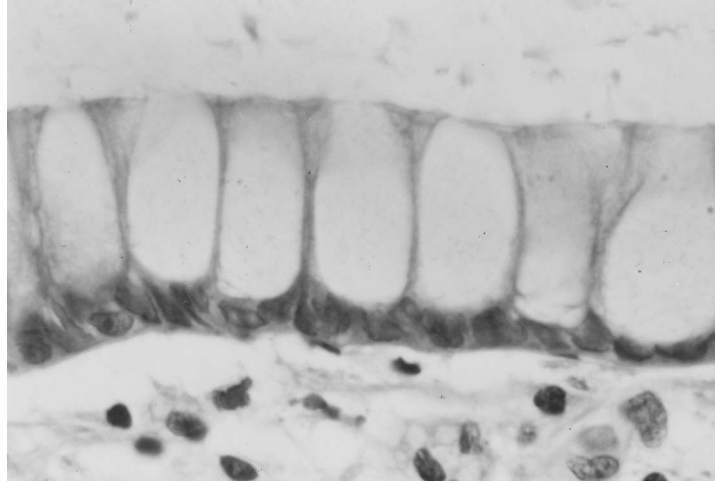


Fig. 1. Photomicrograph of the perpendicular section of the colon epithelial cells. The cytoplasm of each epithelial cell is filled by mucin, white in the micrograph, and its nucleus is locating at the lower basis. The upper horizontal line is the surface of each epithelial cell, and the lower line is the basal line towards the extracellular matrix.

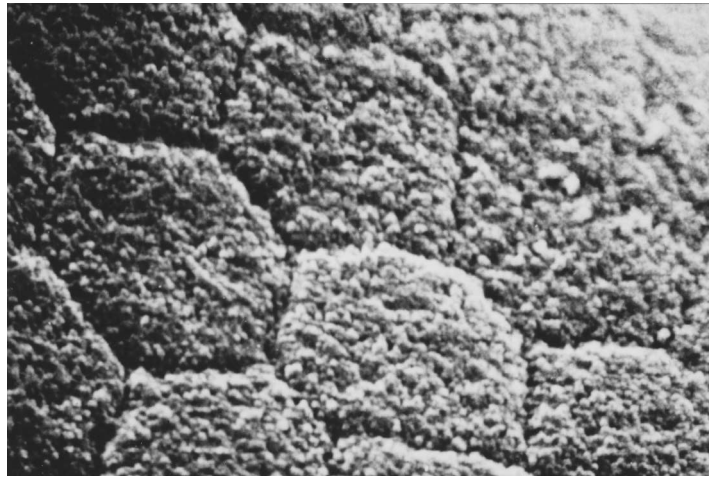


Fig. 2. Oblique view image of the surface of the small intestinal epithelial cells by scanning electron microscope. Most of the cell surfaces are hexagons.

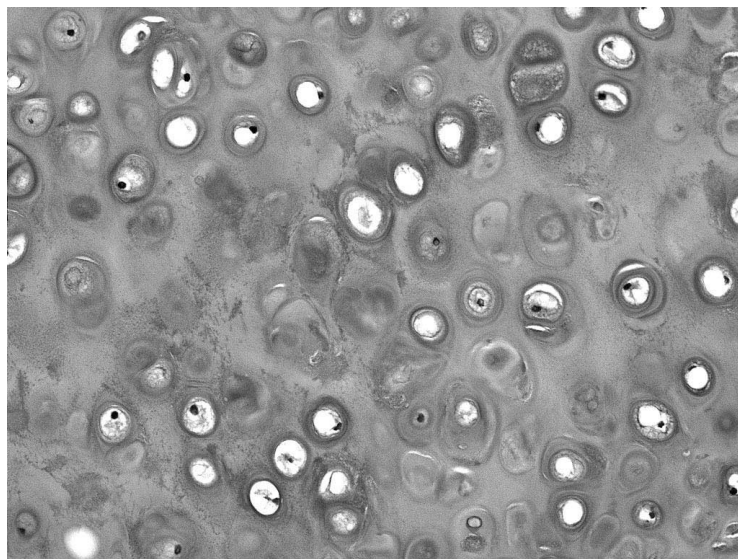


Fig. 3. Photomicrograph of the cartilage. Round chondrocytes are distributed in the extracellular matrix.

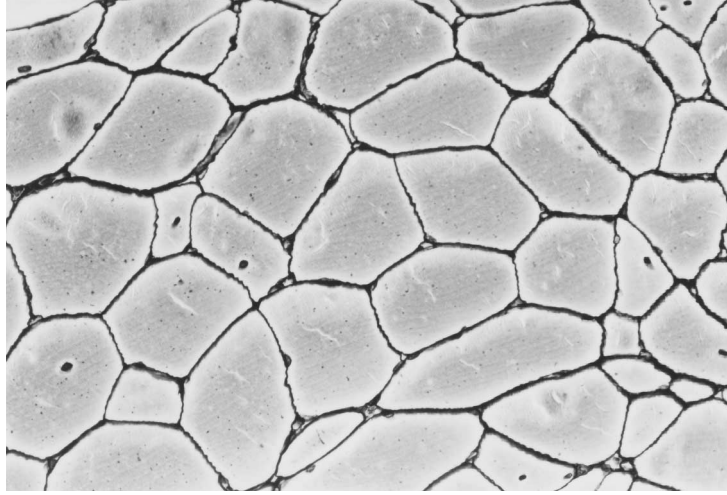


Fig. 4. Photomicrograph of skeletal muscles in cross section.

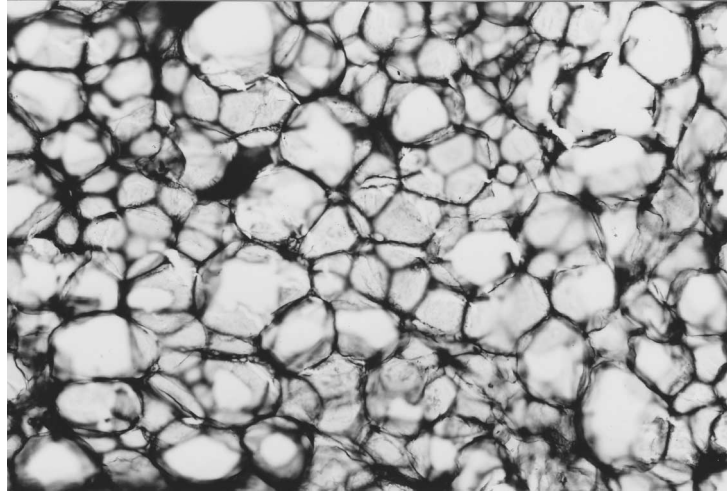


Fig. 5. Photomicrograph of fat tissue in a thick section of a healthy person. The extracellular matrix between fat cell membranes is stained black.

have

$$\begin{aligned} F - E + V \\ &= \Sigma f_i - (1/2)\Sigma i \cdot f_i + (1/3)\Sigma i \cdot f_i \\ &= \Sigma f_i - (1/6)\Sigma i \cdot f_i = \chi. \end{aligned}$$

Then, we have

$$\begin{aligned} \Sigma(6 - i) \cdot f_i &= 6\chi, \\ \Sigma(6 - i) \cdot p_i &= 6\Sigma p_i - \Sigma i \cdot p_i \\ &= 6 - \langle i \rangle = 6\chi/F, \end{aligned}$$

where $\langle i \rangle$ is the mean number of edges of the polygons. The larger the number of polygons (F) grows, the smaller $6\chi/F$ becomes, and $\langle i \rangle$ converges to 6.

2. 3D Shape of Cells in the Tissue

The fat tissue is mainly composed of fat cells, and a few fibers and vessels. The fat cell contains much lipid in the cytoplasm (material within cells), and then its nucleus is compressed to the cell margin near the cell membrane. Fat cells of healthy persons fill up the space in the fat tissue,

and their shapes become polyhedra (Fig. 5). Fat cells of malnutritional persons become spherical and are discretely distributed in the gelatinous matrix, because of exhaustion of lipid (Fig. 6). The spherical cell shape is caused by surface tension like the case of blood cells.

2.1 Why tetrakaidecahedron predominates in fat cells?

We assume that one type of regular polyhedra with the same size is filling the 3D space, and every face contacts precisely with other polyhedron's face. For the space-filling regular polyhedra the following equation is satisfied (Coxeter, 1989b),

$$\sin(\pi/p) \cdot \sin(\pi/r) = \cos(\pi/q), \quad (2)$$

where p is the number of edges of each face of a regular polyhedron, q the number of edges or faces joining each vertex in the polyhedron, r is the number of regular polyhedra joining one edge in the 3D arrangement. The only one combination of integers larger than 2 satisfying Eq. (2) is $p = 4, q = 3, r = 4$, which is the case of cubes piled along the cubic lattice.

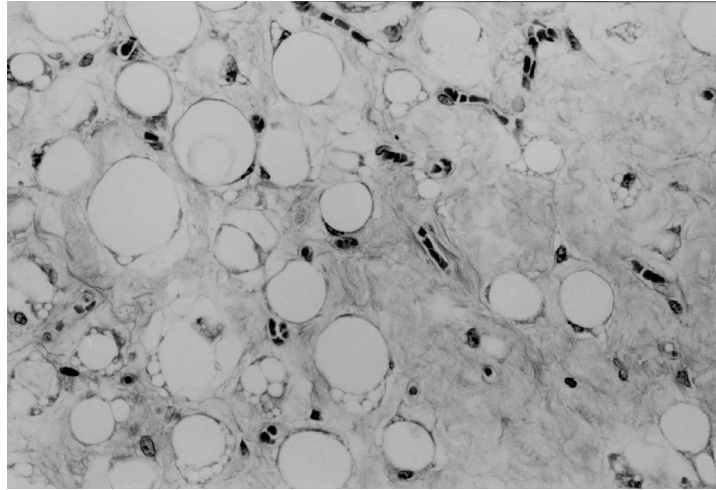


Fig. 6. Photomicrograph of fat tissue of a malnourished person. Fat cells become spherical and are distributed discretely in the gelatinous extracellular matrix.

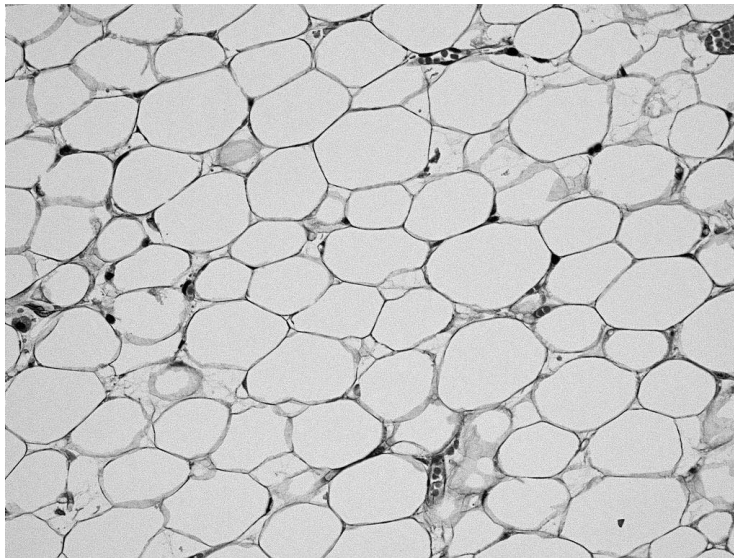


Fig. 7. Photomicrograph of fat tissue in a thin section of a healthy person. Three border-lines of fat cells join one point in histological cross section.

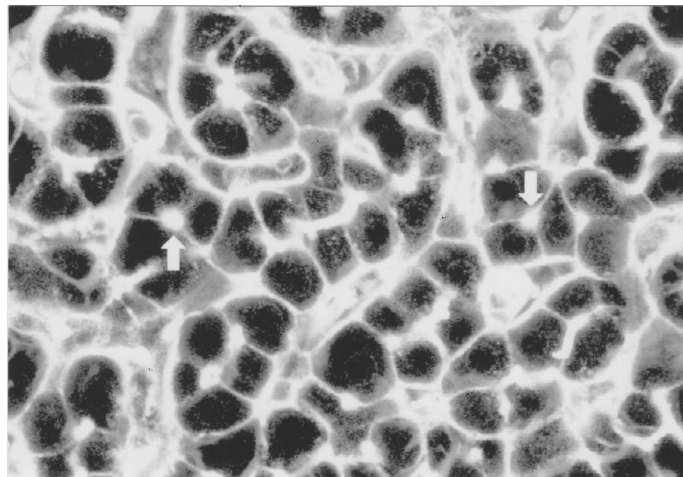


Fig. 8. Micrograph of thick liver tissue by confocal laser scanning microscopy. The white arrows present bile canaliculi.

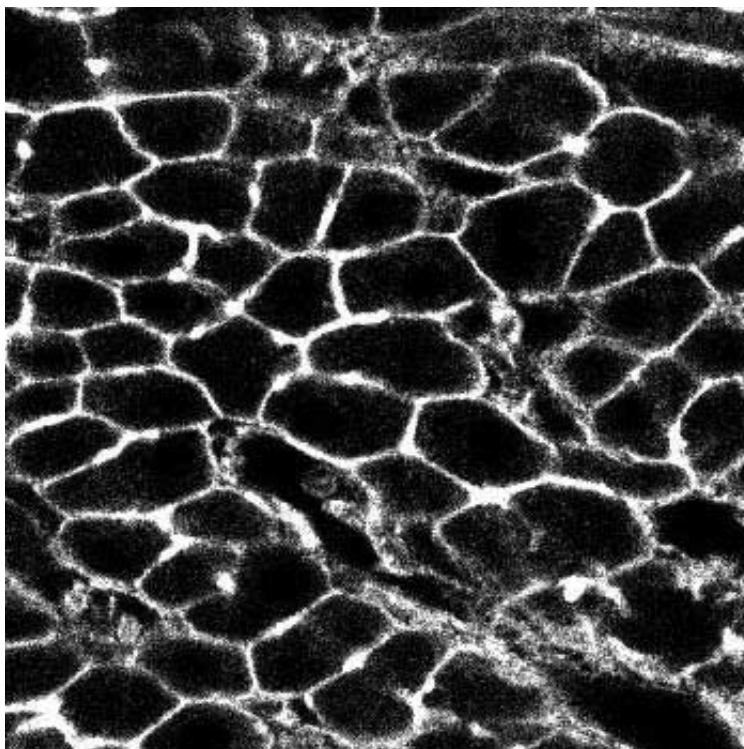


Fig. 9. Micrograph of liver parenchyma by confocal laser scanning microscopy.

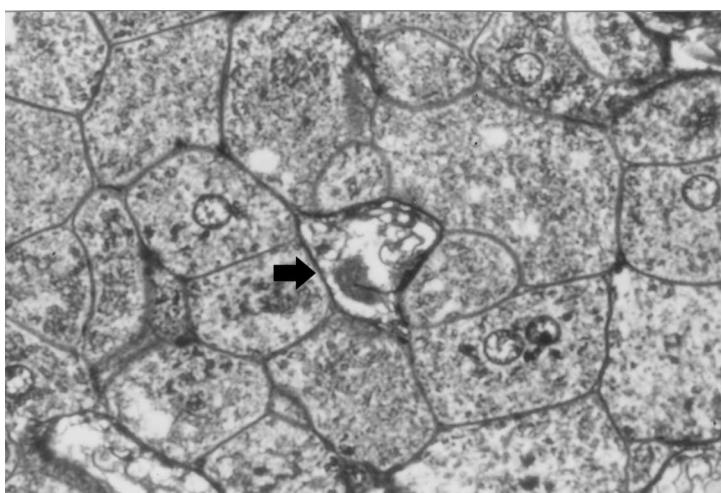


Fig. 10. Photomicrograph of liver tissue. The arrow presents one branch of the sinusoids. The branch goes along faces of the surrounding liver cells.

Another equation (3) comes for a regular polyhedron,

$$pF = 2E = qV \quad (3)$$

where V , E and F are the numbers of vertices, edges, and faces, respectively.

Needless to say, actual fat cells in the tissue are not regular polyhedra, and we have, in general, $q = 3$, $r = 3$, i.e. the number of edges or faces joining each vertex is 3, and the number of cells joining each edge in the packed cells is also 3. Then, three border-lines of fat cells join one point in histological cross section (Fig. 7). This fact means that four cells join at one vertex in the space filling fat cells, owing to dynamical stability. Then, if we put $q = 3$, $r = 3$ into Eq. (2), we obtain $p = 5.1044 \dots$. This means that the

mean number of edges of one face of the space-filling fat cells is $5.1044 \dots$. Put these values into Eq. (3) and Euler's formula (4) (Coxeter, 1989c),

$$F - E + V = 2, \quad (4)$$

hence we obtain $F = 13.398 \dots$. Thus, it is shown that the mean number of faces of space-filling fat cells is $13.398 \dots$.

Kajita (1980) reported of a statistical computer analysis of space division, using random packing of spheres and Voronoi polyhedron (Suwa, 1981), and of its geometrical consideration. His study showed the predominance of tetrakaidehedra and pentagonal faces, and values of F varied from 13.5 to 13.6, and those of p from 5.10 to 5.12 on the average. These two values are very close to those of

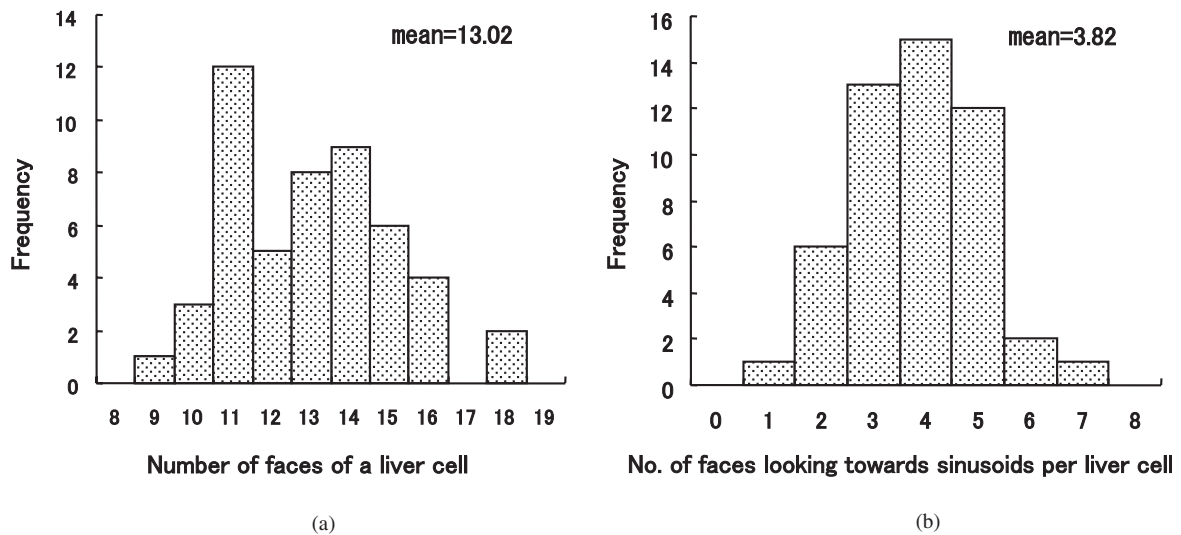


Fig. 11. (a) Histogram of the number of faces of a liver cell. (b) Histogram of the number of faces looking towards sinusoids per liver cell.

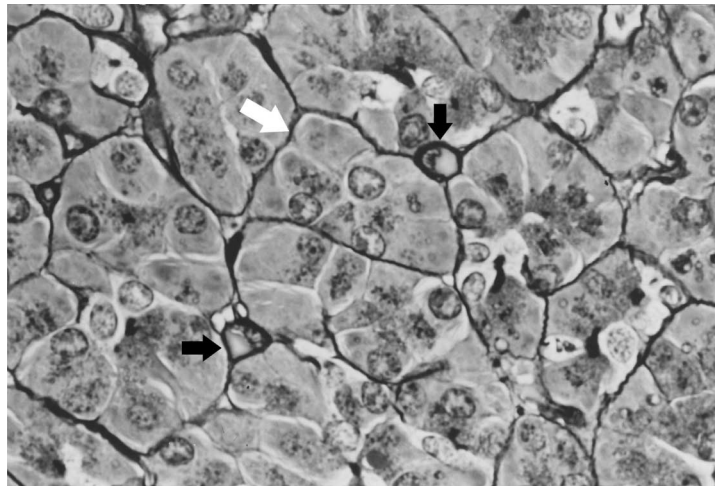


Fig. 12. Photomicrograph of pancreas. Pancreatic tissue is filled by acini, encased by black lines. The white arrow presents an acinus, composed of pleural cells. The black arrows present microvessels, going along the edge of the pancreatic acini.

the fat cells obtained above.

2.2 Liver cell as a unique epithelial cell

Liver cells are epithelial, but have a unique shape and a unique cell arrangement. The liver cell is a glandular epithelial cell that produces and excretes bile (fluid secreted by liver cells). Each liver cell must play the role of not only a glandular epithelial cell but also a ductal epithelial cell, because there is large distance between the liver cell and interlobular bile duct. Minute canals, in which bile flows from liver cells to interlobular bile ducts, are called bile canaliculi. Bile canaliculi run between liver cells throughout the hepatic lobules. As a rule established by observation, a single canaliculus runs between each adjacent pair of liver cells. The diameter of the bile canaliculi is extremely smaller than the size of liver cells, and the lumina of the canaliculi have no influence on the shape and arrangement of liver cells (Fig. 8).

Liver cells fill the space between sinusoids, 3D networks of small vessels, throughout the hepatic lobules, and

liver cells form liver cell plates with 3D networks. The shape of liver cells is polyhedral. Some faces of each liver cell look towards the sinusoids, and the remaining faces front adjacent liver cells. The liver lobule is therefore composed of two structures, i.e. liver cell plates and sinusoids, and this is different from fat tissue. The volume fraction of liver cell plates and that of sinusoids are about 80% and 20% of the liver lobules, respectively.

2.3 How many faces each liver cell has in average?

The present author made an experiment to measure the average number of faces of liver cell. The human normal liver tissue labeled by rhodamine phalloidin was used, and liver cell membranes of fifty cells were observed by confocal laser microscopy at intervals of $1.013 \mu\text{m}$ in thickness (Fig. 9). The diameter of each branch of sinusoids was similar to the size of liver cells, and the sinusoids were found to go along faces of the cells (Fig. 10). Eleven-sided liver cells predominate, and the mean number of faces of liver cells was 13.02. On the other hand, the cells with four faces

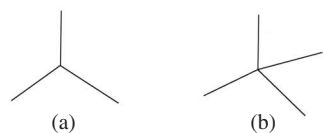


Fig. 13. (a) Illustration of three cells meeting at one vertex on a plane. (b) Illustration of four cells meeting at one vertex on a plane.

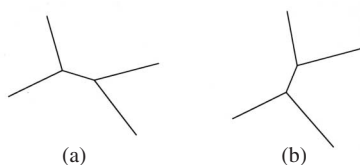


Fig. 14. Illustrations (a), (b) transformed from the unstable pattern in Fig. 13b.

looking towards sinusoids predominated and the mean number of faces looking towards sinusoids per liver cell is 3.82 (Figs. 11a and 11b) (Shimizu *et al.*, 1998).

The mean number of faces, 13.02, is close to that of fat cells obtained based on the topology and that of Voronoi polyhedra by the statistical computer simulation. But, the predominant value did not agree with the theoretical one. In the topological analysis or the computer simulation, the examined space was divided by a single kind of cells. On the other hand, the human liver is filled up by two structural elements, i.e. liver cells and sinusoids, this may influence on the predominant number of faces.

In conclusion, when cells fill up the space, the mean number of faces of each cell is close to 14, regardless of type of cells, such as non-epithelial cells or epithelial cells. And when polyhedra fill up the space, the mean number of faces of each polyhedron is close to 14, regardless of type of the used method, such as topology or computer simulation.

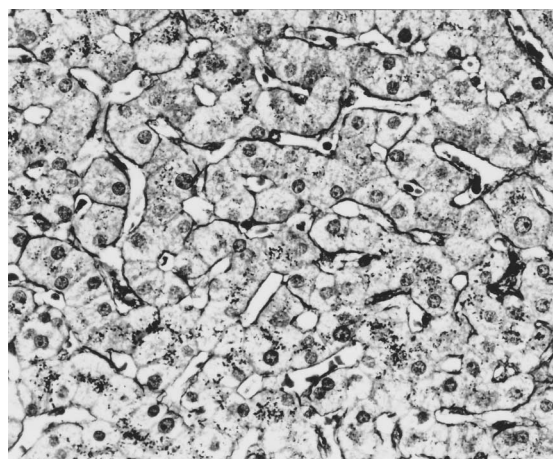
3. Who Determines the Arrangement of Blood Vessels?

A cell in general means a small, more or less closed space or room. In biology a cell means the smallest unit of protoplasm (living contents in a cell) capable of independent existence. An acinus (small unit) of the pancreas (an organ) is composed of plural cells, and it is a more or less closed space, then we can consider a pancreatic acinus as a cell (Fig. 12). We regard a cell as a general meaning in the following discussion.

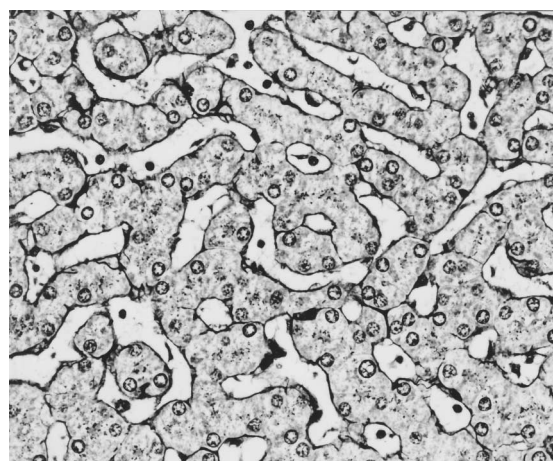
When cells fill up some part of a plane, it is dynamically stable if three cells meet at one vertex (Fig. 13a). Four cells rarely meet at one vertex (Fig. 13b), because this arrangement is dynamically unstable, and transforms into a state with two vertices at which three cells meet (Figs. 14a and b).

3.1 Positional relationship between cells and blood vessels

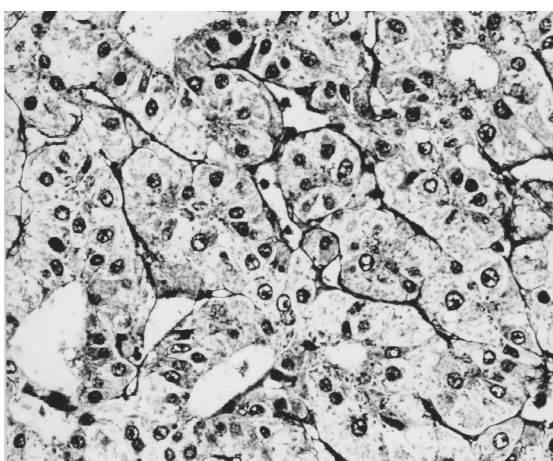
When many 3D cells fill up some part of the space, four cells meet at one vertex and three cells meet at one edge, this is dynamically a stable condition. If the diameter of blood vessels is smaller than the size of cells, the vessels go along the position of edges of the cells (Fig. 12). It is



(a)



(b)



(c)

Fig. 15. (a) Photomicrograph of a normal liver. (b) Photomicrograph of a cirrhotic liver. (c) Photomicrograph of a hepatocellular carcinoma.

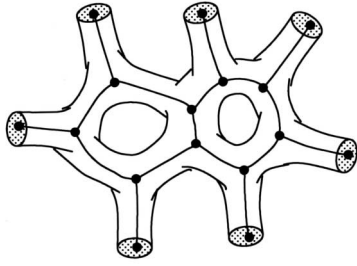


Fig. 16. Construction of a node-branch network corresponding to a multiply connected solid branches. Cycle rank \mathcal{P}_1 (number of independent cycles) is calculated by Euler-Poincaré formula: $\mathcal{P}_1 = \mathcal{P}_0 - \mathcal{n} + \mathcal{b} = 1 - 16 + 17 = 2$.

guessed that the pressure between cells forces small vessels move to intercellular spaces such as the position along the edges.

There is an observation that small blood vessels going along the cell edges do not occupy all edges of cells but use only some edges. Some researchers speculate on this reason, but it is not confirmed. The length distribution of small vessel branches therefore represents somewhat that of cell edges.

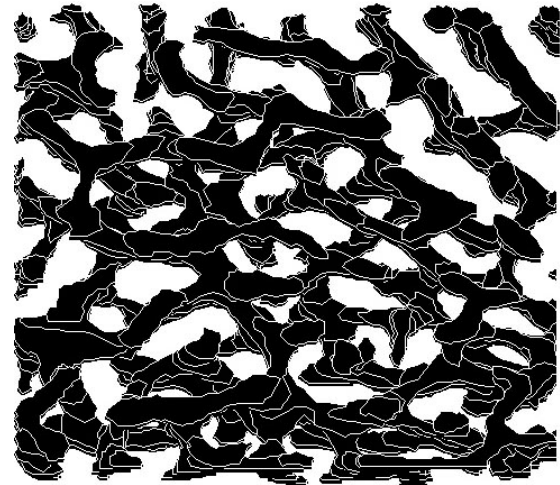
It is noted here that no significant difference was observed between space-filling cells with DNA and those without DNA in distributions of the numbers of faces and the numbers of edges of particular faces (Lewis, 1923, 1933; Matzke, 1939; Kajita, 1980). This fact should mean that DNA has no effect on the shape of the cells. By the way there are few reports on dimensions, such as edge lengths or face areas, of the space-filling cells. DNA can of course order the proliferation (increase in number) of small vessels or endothelial cells at some stage. But DNA has no influence on where the small vessels go along or how long the edges of the vessels are. Therefore, it is physical laws that determine these things statistically.

4. Pathologic Change of the 3D Structure of Hepatic Sinusoids

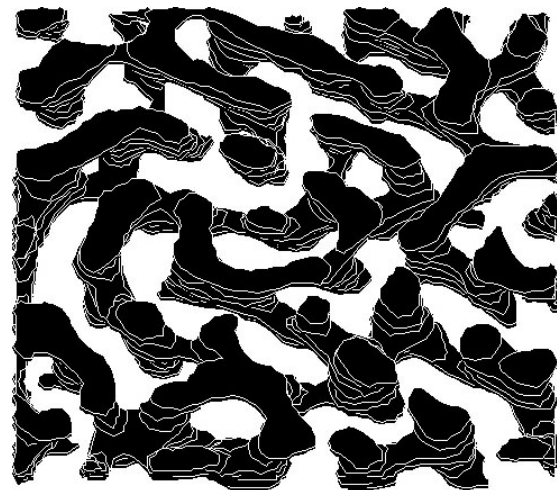
Liver cells exchange substances with the blood in the sinusoids. The lining of the sinusoids consists of a thin layer of endothelial cells and fixed macrophages, the stellate cells of Kupffer. The space between the sinusoids is light microscopically filled up by liver cell plates in normal human liver (Fig. 15a). This condition is the same in cirrhotic liver (Fig. 15b). In hepatocellular carcinoma (HCC), carcinoma cells are filling up the space between the sinusoids (Fig. 15c). The liver cell plates are occupying the major part of the liver lobules, and their 3D structure is very complicated, so that we choose the sinusoids as an object of study that are a complementary set of the liver cell plates, and their 3D structure can be handled more easily than that of the liver cell plates.

4.1 Topological analysis of the 3D sinusoid structure

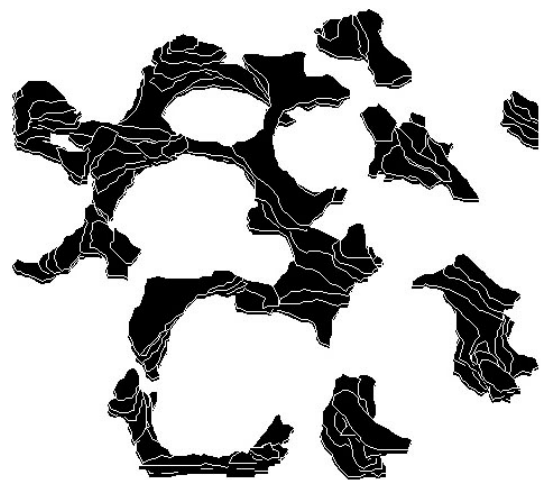
The 3D sinusoid structure can be treated much more easily if we replace each solid branch of the sinusoids by a one-dimensional complex (node-branch network) of topologically equal connecting relationship (Fig. 16). The node-



(a)



(b)



(c)

Fig. 17. Plane-type reconstruction figures of the sinusoids in seven serial sections by a computer system. (a) Normal liver. (b) Cirrhotic liver. (c) Hepatocellular carcinoma.

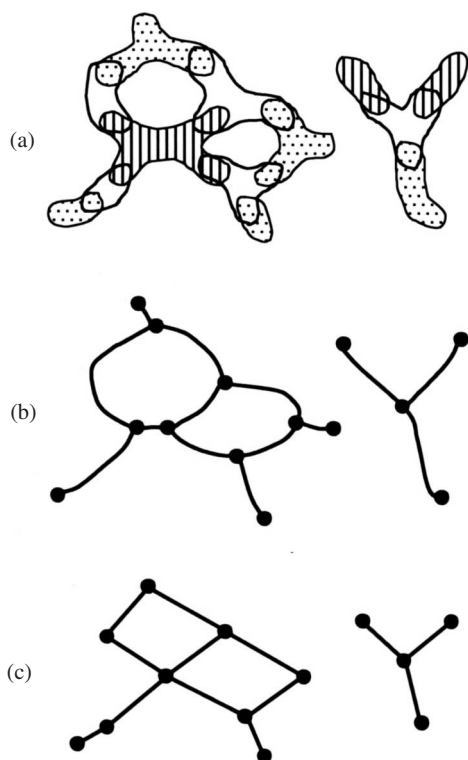


Fig. 18. Schemas illustrating the relationship between the original network and the network figure obtained using the author's computer system. (a) A reconstructed figure of sinusoids in three serial sections, by direct viewing from above. The sinusoids in the first section are shown by the striped areas; those in the second section by the white areas, and those in the third section by the dotted areas. (b) A node-branch network corresponding to the skeleton of (a), that is, the original network. $p_1 = p_0 - n + b = 2 - 14 + 14 = 2$. (c) A network figure of (a) obtained using the author's computer system. The nodes in (c) denote the sinusoidal segments in the serial sections in (a). $p_1 = p_0 - n + b = 2 - 12 + 12 = 2$. In the algorithm, the number of nodes (n) and number of branches (b) in (c) were different from those of the original network in (b). However the number of connected components (p_0) and number of independent cycles (p_1) in (c) are identical with those of the original network in (b).

branch network of a sinusoid network is formed by putting a line in each sinusoid branch and by putting a node at each joining point and at each endpoint of the sinusoid branches. Topological analysis can then be easily performed by means of an invariant, i.e. *cycle rank* p_1 . p_1 may be defined as the number of independent cycles (Harary, 1972). Let n be the number of nodes and b the number of branches, then p_1 can be determined by Euler-Poincaré formula

$$n - b = p_0 - p_1, \quad (5)$$

where p_0 denotes the number of connected components in the network. An example of calculating the p_1 of a network is shown in Fig. 16. p_0 and p_1 are quantities termed the *0th and 1st Betti numbers*, respectively. The *1st Betti number* is a number of independent cycles (Fig. 16), and means the complexity of the figure.

4.2 Computer-aided reconstruction

The computer-aided reconstruction system was employed, which was developed by Rise Co. Ltd. (Sendai,

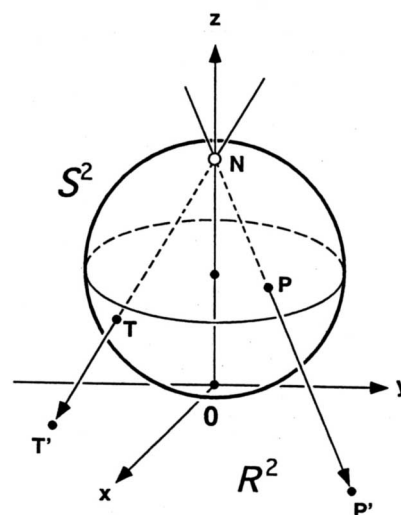


Fig. 19. $S^2 - \{N\}$ and R^2 are homeomorphic because there exists a continuous bijective map f of $S^2 - \{N\}$ onto R^2 such that the inverse map f^{-1} is also continuous. That is $S^2 - \{N\} \cong R^2$.

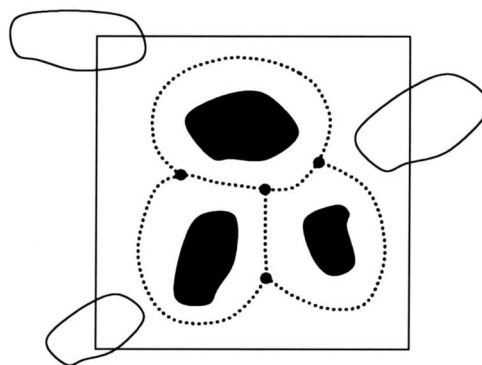


Fig. 20. Schema illustrating the relationship between the number of sinusoidal profiles and the first Betti number of the 3D hepatic cell plates. Black islands are the counted profiles that are fully enclosed by hepatic cell plates. Broken lines show handles of the 3D hepatic cell plates.

Japan) and enables 3D image reconstruction from serial tissue sections by the use of a personal computer. A square test area with side of $200 \mu\text{m}$ was set in each serial tissue section, and the outlines of the sinusoids contained in the square areas were fed into computer through digitizer.

The reconstruction program consists of two types of jobs, a plane type (Figs. 17a, b and c) and network type. By means of the network reconstruction program, when a segment (sinusoid lumen) overlaps with another segment in an adjacent tissue section, then a straight line is drawn between each barycenter of the two segments (Fig. 18). After n , b , and p_0 are confirmed, p_1 can be calculated. This computer system also makes it possible to calculate the volume of the structure from 2D images obtained from histological sections.

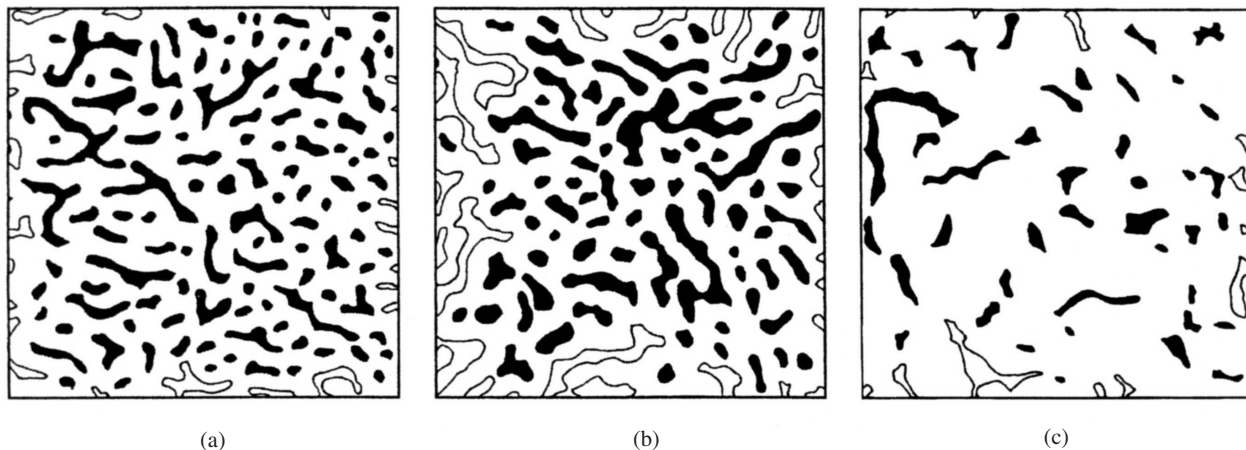


Fig. 21. Sinusoidal profiles in a given area, $400 \times 400 \mu\text{m}^2$ in size, on a single tissue section. Black islands are the counted profiles. (a) Normal liver. (b) Cirrhotic liver. (c) Hepatocellular carcinoma.

4.3 3D structural change of sinusoids in cirrhosis and hepatocellular carcinoma

The mean (\pm SD) p_1 of the sinusoids in the examined tissue, $200 \times 200 \times 80 \mu\text{m}^3$ in size, was 181.2 ± 23.9 in the normal liver, 84.9 ± 19.1 in the cirrhotic liver (Shimizu, 1993), and 46.5 ± 33.0 in HCC (Shimizu, 1996). There was a statistically significant difference in p_1 of the sinusoids in the same size tissue between any two groups in the three ones. The mean (\pm SD) sinusoid volume in the tissue was $6.43 \pm 0.55 (10^5 \mu\text{m}^3)$ in the normal liver, $6.11 \pm 1.33 (10^5 \mu\text{m}^3)$ in the cirrhotic liver (Shimizu, 1993), and $5.43 \pm 1.94 (10^5 \mu\text{m}^3)$ in HCC (Shimizu, 1996). There was no statistically significant difference in the sinusoid volume in the same size tissue between any two groups in the three ones.

5. Which are More Complex, Sinusoids or Liver Cell Plates?

The liver tissue is light-microscopically filled up by the 3D network of liver cell plates and that of sinusoids. Which network is more complex? In order to answer this question we must first explain one theorem in the topology.

The 1D sphere S^1 is a circumference in the 2D Euclidian space (R^2) and the 2D sphere S^2 is a surface of a solid sphere in the 3D Euclidian space (R^3). Let $S^1 - \{M\}$ be a figure of S^1 from which a point M is removed, and $S^2 - \{N\}$ a figure of S^2 from which a point N is removed (Fig. 19). In topology two figures X and Y are called homeomorphic, i.e. $X \cong Y$, if there exists a continuous mapping f of X onto Y such that the inverse map f^{-1} is also continuous. Then $S^1 - \{M\}$ and R^1 are homeomorphic, $S^2 - \{N\}$ and R^2 are also homeomorphic. Therefore, $S^1 - \{M\} \cong R^1$, $S^2 - \{N\} \cong R^2$.

Similarly, let $S^3 - \{Q\}$ be a figure of S^3 from which a point Q is removed, then $S^3 - \{Q\} \cong R^3$. The figure of S^3 is identical with the figure of $R^3 \cup \{Q\}$, and the figure of S^3 cannot be embedded in R^3 , but can be embedded in R^4 . We can sensuously consider that S^3 is almost the same as R^3 where we live, but the space R^3 is devoid of a point of infinity.

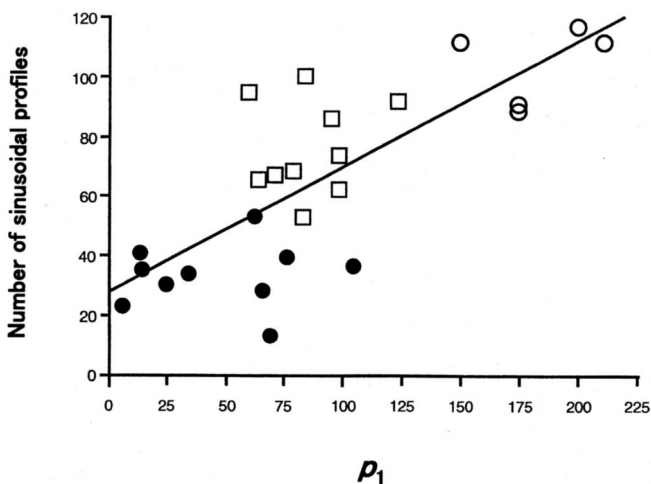


Fig. 22. Regression line of p_1 versus number of sinusoidal profiles in a given area. Open circles (\circ) show normal livers. Open squares (\square) show cirrhotic livers. Closed circles (\bullet) show hepatocellular carcinomas. Number of sinusoidal profiles = $0.42p_1 + 27.96$. Correlation coefficient = 0.77.

5.1 Alexander duality theorem

Let S^n be an n -sphere and Π be a subpolyhedron of S^n . The p -th Betti number of figures is denoted by R_p . Then, according to Alexander, between the Betti numbers of the closed polyhedron Π and those of the open polyhedron $S^n - \Pi$ there takes place the duality relation (Lefschetz, 1949)

$$R_p(S^n - \Pi) = R_{n-p-1}(\Pi) + \delta_{p,0} - \delta_{p,n-1}, \quad (6)$$

where the $\delta_{i,j}$ are Kronecker deltas (when $i = j$, $\delta_{i,j} = 1$, when $i \neq j$, $\delta_{i,j} = 0$). Put $p = 1$, $n = 3$ into the formula (6), $\delta_{1,0} = \delta_{1,2} = 0$, and then

$$R_1(S^3 - \Pi) = R_1(\Pi). \quad (7)$$

5.2 Which are more complex, sinusoids or liver cell plates?

The liver tissue is filled up by sinusoids and liver cell plates, let the sinusoids be looked upon as Π , then $S^3 - \Pi$ corresponds to the liver cell plates. Here we assume that the outside of the examined domain is filled up only by liver cell plates. Then the formula (7) shows that the p_1 of sinusoids is the same as that of liver cell plates. The complex degree of sinusoids is therefore the same as that of liver cell plates topologically.

5.3 2D index estimating the complex degree of 3D structure

Reconstruction study from serial tissue sections requires much time and energy, not being easily applicable to routine histopathological diagnosis. Based on the results from the previous reconstruction study and resorting to the principles of topology, we now propose a method to use an index that can easily be evaluated from a single tissue section and indicates the degree of complexity of the 3D sinusoidal structure. The index, called "numerical density" in stereology, is the number of sinusoidal profiles (cross sections) in a given area on a single tissue section.

Each segment of sinusoids has almost straight, having a tubular structure, and no knots are found in normal liver, cirrhotic liver, or HCC. There are in the network very few sprouts or blind ends; in other words, each sinusoidal segment connects with others at its bilateral ending points (Motta *et al.*, 1978). One may see therefore that each sinusoidal profile appearing in a 2D section corresponds to a "handle" of hepatic cell plates in 3D space, if the profile is not cut at the examined area's margin (Fig. 20).

The number of sinusoidal profiles, or 2D index, in a given square area $400 \times 400 \mu\text{m}^2$ on a single tissue section was counted (Fig. 21). The mean number of sinusoidal profiles (\pm SD) was 104.2 ± 13.1 in 5 normal livers, 77.0 ± 15.8 in 10 cirrhotic livers (Shimizu *et al.*, 1994) and 34.0 ± 10.7 in 10 HCCs (Shimizu and Suda, 1998). The differences between the three groups were statistically significant ($P < .01$). The number of sinusoidal profiles was approximately linearly related to the p_1 , a 3D structural index, of the sinusoids. The correlation coefficient = .77 (Fig. 22).

The number of profiles in a given area on a single section of a 3D structure is not always an effective index for structural analysis if the structure has anisotropic distribution, has many sprouts or consists of curved branches. However, the sinusoidal networks from normal, cirrhotic liver and from HCC proved to be isotropic in its distribution in 3D space. In addition, they had very few sprouts and were composed of almost straight, tubular segments. Therefore, the number of profiles in a given area on a tissue section was considered to serve as a useful index in structural analysis (Shimizu *et al.*, 1994). There is, however, an exception, where the sinusoidal profile does not correspond to a handle of hepatic or HCC cell plates. This case occurs when the sinusoidal network is cut just the branching point and appears in the tissue section. The number of branching points con-

tained in a certain volume of tissue is larger in normal liver than in cirrhotic liver, and the number is much less in HCC. This suggests the number of sinusoidal profiles may have been more underestimated that in normal liver than in the cirrhotic liver and that in the cirrhotic liver the number may have been more underestimated than in HCC. In spite of this situation, the 2D index, or the number of sinusoidal profiles in a given area on a single tissue section, is therefore useful for estimating the degree of complexity of the 3D sinusoidal network.

In routine histopathologic examination of needle biopsy specimens (removed tissues for microscopic diagnosis) from cirrhotic liver, the diagnosis of cirrhosis is not always possible because of the small size of the biopsy specimen, which often fails to contain septal tissues (fibrous bands) characteristic of cirrhotic changes. In such cases, the 2D index may be effective for strengthening a diagnosis of cirrhosis. It is thus anticipated that application of the 2D index would facilitate rapid characterization of the 3D structure of isotropically distributed capillaries and other 3D network structures in other organs and their changes in various pathologic conditions.

References

- Coxeter, H. S. M. (1989a) *Introduction to Geometry*, 2nd ed., John Wiley & Sons, Inc., NY, pp. 373–374.
- Coxeter, H. S. M. (1989b) *ibid.*, pp. 396–412.
- Coxeter, H. S. M. (1989c) *ibid.*, pp. 152–154.
- Harary, F. (1972) *Graph Theory*, Addison-Wesley, Reading, MA.
- Kajita, A. (1980) On the shape of the tissue unit I. Statistical-geometrical model of the cell-aggregates, *J. Tokyo Women's Med. College*, **50**, 1053–1063 (in Japanese).
- Lefschetz, S. (1949) *Introduction to Topology*, Princeton Univ. Press, NJ, pp. 204–206.
- Lewis, F. T. (1923) The typical shape of polyhedral cells in vegetable parenchyma and the restoration of that shape following cell division, *Proc. Am. Acad. Arts Sci.*, **58**, 537–552.
- Lewis, F. T. (1933) The significance of cells revealed by their polyhedral shapes, with special reference to precartilagelike, and a surmise concerning nerve cells and neuroglia, *Proc. Am. Acad. Arts Sci.*, **68**, 251–284.
- Matzke, E. B. (1939) Volume-shape relationships in lead shot and their bearing on cell shape, *Am. J. Bot.*, **26**, 288–295.
- Motta, P., Muto, M. and Fujita, T. (1978) *The Liver: An Atlas of Scanning Electron Microscopy*, Igaku-Shoin, Tokyo, pp. 130–143.
- Shimizu, H. and Suda, K. (1998) 2-D index as a measure for estimating the complexity degree of 3-D sinusoidal structures in the normal and cirrhotic liver and in hepatocellular carcinoma, *Analytical and Quantitative Cytology and Histology*, **20**, 526–528.
- Shimizu, H. and Yokoyama, T. (1993) Three-dimensional structural changes of hepatic sinusoids in cirrhosis providing an increase in vascular resistance of portal hypertension, *Acta Pathologica Japonica*, **43**, 625–634.
- Shimizu, H. and Yokoyama, T. (1994) Two-dimensional index as a measure to estimate the complexity degree of three-dimensional hepatic sinusoidal structure, *Forma*, **9**, 29–36.
- Shimizu, H., Suda, K. and Yokoyama, T. (1996) Difference in the three-dimensional structure of the sinusoids between hepatocellular carcinoma and cirrhotic liver, *Pathology International*, **46**, 992–996.
- Shimizu, H., Sueyoshi, N., Sakurai, T., Sonoue, K. and Tanemura, M. (1998) How many faces does each liver cell have in human?, *Bulletin of the Society for Science on Form*, **13**, 101–102 (in Japanese).
- Suwa, N. (1981) Supracellular structural principle and geometry of blood vessels, *Virchows Arch. (Pathol. Anat.)*, **390**, 161–179.